I&EC research
Industrial & Engineering Chemistry Research

pubs.acs.org/IECR
Article

Kinetic Studies of Gas Hydrates for CO_2 Capture in the Presence of Nanoparticles

Phakamile Ndlovu, Saeideh Babaee,* Paramespri Naidoo, and Kuveneshan Moodley

Cite This: *Ind. Eng. Chem. Res.* 2024, 63, 3867−3879

ABSTRACT: High levels of CO_2 in the atmosphere have led to drastic climate changes, and along with the threat of the impact of a two or more-degree temperature rise, intensive research on carbon capture has opened new and promising avenues. The hydrate-based CO_2 capture method is an environmentally friendly approach, and the application of additives such as nanoparticles has shown a promising avenue for increasing the rate of hydrate formation. This research delved into the impact of both nano- and microparticles on the kinetics of CO_2 hydrate formation. The selected chemical substances included nanoparticles and nanoplatelets of aluminum oxide, copper oxide, and graphene, respectively, as microparticles of graphite powder, zinc oxide, and magnesium nitrate hexahydrate. Additionally, the study examined the influence of temperature and pressure through experimental means and the kinetics affecting the gas hydrate formation such as induction time, storage capacity, gas consumption, water conversion percentage, and the ratio of gas consumed to moles of water. For this investigation, nanofluids with concentrations of additives ranging from 0.1 to 1.2 wt % including 0.05 wt % sodium dodecyl sulfate, were employed. In all experiments involving additives, the initial conditions for temperature and pressure were set at 275.8 K and 3.41 MPa, respectively. The study's results demonstrate that nanoparticles enhance the kinetics of CO_2 hydrate formation, leading to higher storage capacity, increased water conversion, and a faster rate of gas absorption. Additionally, in hydrate formation, the use of nanoparticles reduced the induction time. These findings are promising for the potential application of nanoparticles in the storage of CO_2 gas within gas hydrates.

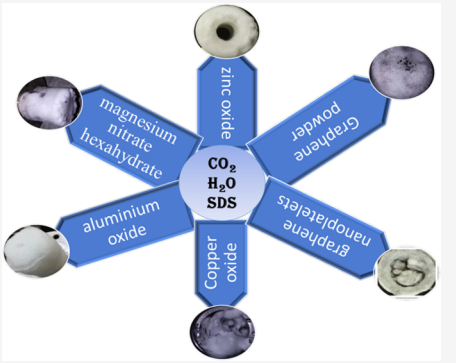

1. INTRODUCTION

Global warming has been exacerbated by high atmospheric concentrations of carbon dioxide (CO_2). According to Solomon et al.,[1] a significant amount of energy and automotive power is produced from fossil fuels, which contributes to these emissions. The two sources of carbon dioxide emanating into the atmosphere are natural processes that account for most of the atmospheric carbon dioxide, and these are balanced out by forests and oceans, which serve as natural carbon sinks. Another source is based on man-made carbon dioxide. This includes, among others, the use of fossil fuels in vehicles and industrial activities.[2] Three conventional approaches for capturing carbon dioxide emissions from fossil fuel furnaces are oxyfuel combustion, postcombustion, and precombustion. Precombustion capture involves preparing the fossil fuel before it is burned in order to eliminate the organic components responsible for CO_2 emissions. This process entails burning the fossil fuel in a gasifier with limited oxygen, resulting in the production of syngas, which consists of carbon monoxide (CO) and hydrogen (H_2), as a form of pretreatment. Postcombustion capture is a procedure that uses adsorption or absorption technologies to remove CO_2 from the flue gas shortly after combustion.[3,4] In absorption, a liquid phase is used to extract CO_2 from the flue gas, whereas a solid absorbent is used in adsorption to attach CO_2 to its surface. The sorbent is then regenerated by heating, depressurization, and/or stripping.[5] The shortcomings of existing technologies, including their high energy demands and less-than-optimal efficiency, have prompted the search for alternative approaches to capture CO_2.[6] Other technologies are being researched for carbon capture from flue gas; these include hydrate-based separation, enzyme-based separation, chemical-looping combustion, dual-alkali absorption approach, mixed matrix membrane, and integrated gasification combined cycle (IGCC).[7−9] The conditions required for carbon dioxide hydrate formation are less stringent in comparison to other flue gases.[10] Specifically, at a temperature of 0 °C, the pressure needed for CO_2 gas hydrate formation is 3.8 (MPa),[11] while for N_2, the gas hydrate formation pressure is 15 MPa,[12] and 10 MPa for O_2,[13] making this technology an excellent choice for CO_2 capture from flue gas.

Received: November 17, 2023
Revised: January 31, 2024
Accepted: January 31, 2024
Published: February 20, 2024

https://doi.org/10.1021/acs.iecr.3c04061
Ind. Eng. Chem. Res. 2024, 63, 3867−3879

Table 1. Details and Descriptions of the Chemicals Used in the Investigation

chemicals	description	CAS number	formula	supplier	purity (vol %)
carbon dioxide	gas	124-38-9	CO_2	Afrox	>99.9
aluminum oxide	<50 nm nanoparticles	1344-28-1	Al_2O_3	Sigma-Aldrich	
copper oxide		1317-38-0	CuO		>90.0
zinc oxide	5 μm powder	1314-13-2	ZnO		
graphene	nanoplatelets	7782-42-5	(GPN)		
graphite	<20 μm powder	7782-42-5	C		
magnesium nitrate hexahydrate	crystals	13 446-18-9	$MgN_2O_6{\cdot}6H_2O$		>99.99
sodium dodecyl sulfate	220−350 nm	151-21-3	$CH_3(CH_2)_{11}OSO_3Na$		>99.0
water[a]			H_2O		

[a]Deionized water obtained from Algae ultrapure water system with conductivity of 0.64 mS/cm.

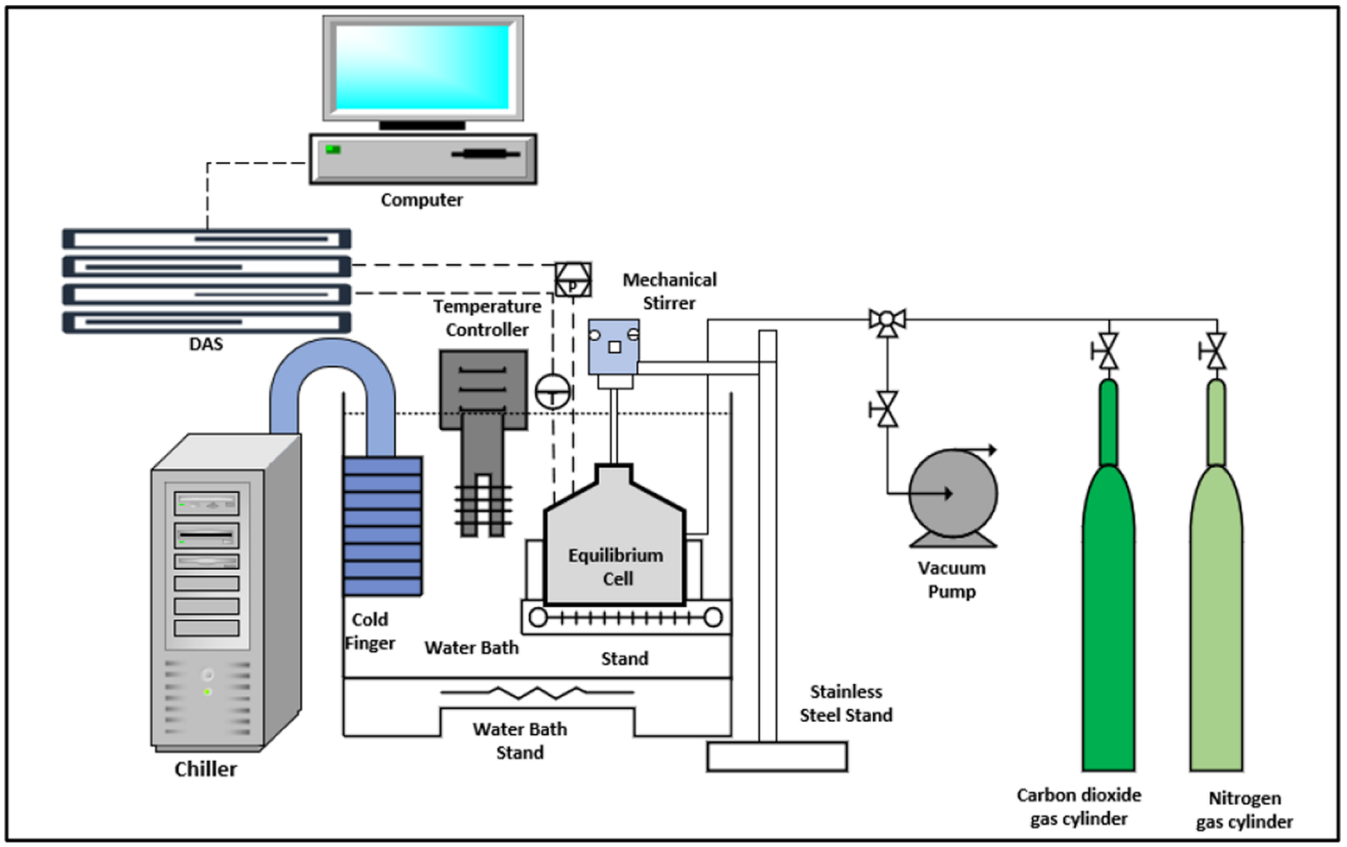

Figure 1. Schematic diagram of the experimental setup used for the measurement of CO_2 hydrate kinetics. (In this diagram, DAS represents Data Acquisition System in a summarized form.)

Gas hydrates have been noted for their substantial gas storage capability, with one cubic meter of gas hydrate potentially holding as much as 164 m^3 of gas at standard room temperature and pressure.[14] Though gas hydrates possess a large storage capacity, the amount of gas storage is inadequate for the hydrate technology to be applied for domestic and industrial purposes. Furthermore, the prolonged process of gas hydrate formation and the substantial time gap between the introduction of the gas into the system and the initial appearance of the hydrate structure (known as the induction period) render the use of gas hydrate technology economically unfeasible. The kinetics of gas hydrates are essential studies in understanding and exploring modifications to the techniques to make the hydrate technology economically viable and possible for large-scale industrial applications.[15] Experimental studies report the use of chemical additives and nanoparticles to improve hydrate storage capacity.[14,16] The application of nanoparticles in CO_2 capture has not yet been investigated in-depth yet. Seo et al.[17] examined how silica nanoparticles could improve the formation of CO_2 hydrates, whereas Masoumi et al.[18] employed iron(II) oxide in the formulation of CO_2 gas hydrates. Soltanieh et al.[19] investigated the formation of CO_2 in the presence of TiO_2 nanoparticles. Firoozabadi et al.[20] utilized Fe_3O_4 with SDS and CTAB in CO_2 gas hydrate formation. The reason for incorporating nanoparticles in hydrate formation is their favorable impact on the thermodynamics and transport phenomena, which improves gas hydrate formation kinetics.[21] Nanofluids pertain to the suspension of nanoparticles within a liquid, which can be substances like water, alcohol, or ethylene glycol.[22] The CO_2-CH_4 system was investigated during the formation of gas hydrates, paying special attention to the rate at which gas was utilized and the total quantity of gas consumed. The study was conducted with the inclusion of nanoparticles like Al_2O_3, SiO_2, Ag, and Cu at

https://doi.org/10.1021/acs.iecr.3c04061
Ind. Eng. Chem. Res. 2024, 63, 3867−3879

concentrations of 0.1, 0.2, and 0.3 wt %. The findings indicated that 0.3 wt % SiO_2 nanoparticles led to an improvement in the quantity of consumed CO_2 gas. Meanwhile, Cu and Al_2O_3 nanoparticles resulted in a 30−65% increase in gas consumption.[23] Zhou et al. conducted experiments to examine the impact of 0.4 wt % graphite nanoparticles on the induction period and gas consumption during the formation of CO_2 gas hydrates. The inclusion of nanoparticles led to an 80.8% reduction in the induction period, and the amount of stored CO_2 improved by 12.8%.[24]

The use of sodium dodecyl sulfate (SDS) has been noted to enhance the absorption of CO_2 gas during gas hydrate formation, acting as a catalyst to speed up the process.[25] Additionally, the combination of SDS and tetrahydrofuran (THF) significantly reduced the time needed for CO_2 gas hydrate development.[26] Furthermore, Choi et al.[27] conducted experiments to develop new adsorbents for the formation of CO_2 gas hydrates at standard pressure in the presence of SDS. They examined how the use of SDS, THF surfactant, and Al_2O_3 nanoparticles influenced both the induction period and the rate of CO_2 hydrate formation. The introduction of Al_2O_3, THF, and SDS was found to enhance the rate of hydrate formation. In separate studies, Moraveji et al.[28] and Aliabadi et al.[29] observed that a concentration of 0.05 wt % SDS was ideal for stabilizing nanoparticles in solution. Higher concentrations were found to eliminate the influence of nanoparticles, while lower concentrations resulted in precipitation. Therefore, this study adopted a concentration of 0.05 wt % SDS.

In this article, the influence of altering the initial temperature within the range of 275.25 to 276.26 K was examined, maintaining a constant initial pressure of 4.07 MPa. Similarly, the impact of varying initial pressure in the range of 3.32−3.41 MPa was investigated while keeping the temperature constant at 275.8 K. These experiments were conducted using deionized water. Subsequently, kinetic analyses were conducted on the formation of CO_2 gas hydrates in the presence of specific nano- and microparticles, maintaining an initial pressure of 3.41 MPa and an initial temperature of 275.8 K. The measured kinetic parameters included storage capacity, induction time, water-to-hydrate conversion, and the rate of gas consumption. The additives selected for this study were CuO and Al_2O_3 nanoparticles, graphite powder, graphene nanoplatelets, ZnO, and magnesium nitrate hexahydrate ($MgN_2O_6{\cdot}6H_2O$) crystals.

2. EXPERIMENTAL METHOD

2.1. Materials. Table 1 provides a list of the substances employed in the study. A precision OHAUS PA4202C top pan balance, accurate to 0.0001 g, was utilized for measuring the additives. The deionized water utilized in this research, produced by the Algae water purification system located in the Chemical Engineering Department Laboratory at the University of KwaZulu Natal, exhibited a conductivity of 0.64 mS/cm.

2.2. Apparatus. Figure 1 displays the experimental apparatus that was used for the study. This equipment has been also used by Ngema et al.,[30] in a hydrate study of fluorinated refrigerants. It comprises a 316 L stainless steel vessel with an upper pressure limit of 10 MPa, a design volume of 52 cm^3, and a usable volume of 36.5 cm^3. The cell's internal stirrer was turned by a motor system that was attached to a shaft with a magnetic tip to accomplish the mixing of reactants. The pressure within the equilibrium cell was monitored by a type 1−10 WIKA pressure sensor with a 0−10 MPa rating. An aluminum block that held the pressure sensor was kept at a constant temperature using a TDGC2 Variac voltage regulator. Temperature was measured using a class A WIKA thermocouple with a 0.08 K precision. An Agilent 34972A data logging device was used to register temperature and pressure data every 5 s. The water/ethyl glycol water bath temperature was maintained using a programmable bath controller Polyscience TXF200 model rated over 243.15−323.15 K and had exterior dimensions of 595 mm × 460 mm × 360 mm. To immerse the cell in the water bath, a mechanical jack was employed to raise and lower the water bath. A rotary vane vacuum pump, specifically the RV12 model, was employed to remove air from the equilibrium cell and connecting lines.[31]

2.3. Procedure. *2.3.1. Sample Preparation.* In order to improve mixing in the fluid, an SDS solution was used to minimize surface tension in the reactant solution. It was assumed that the dissolution of the additives in the solvent occurred up to the saturation point. A 2000 mL volumetric flask containing deionized water and SDS was used to create a 0.05 wt % SDS solution. The production of nanofluid solutions with experimental concentrations was accomplished using this solution. The weight of each nanoparticle was measured with a balance, and subsequently, it was transferred to a 50 mL sterile centrifuge tube. It was then vigorously mixed with the solution for a duration of 5 min using a vortex mixer.[31]

2.3.2. CO_2 Hydrate Formation. Before each experiment began, the cell was opened by removing the top flange. The apparatus was cleaned with acetone, and a 20 cm^3 reaction solution was added to the equilibrium cell, and then it was sealed. The cell was placed in a chilled water bath at a temperature of 275.8 K. It was then subjected to a 5-minute evacuation process to remove any noncondensable gases and air. CO_2 gas was injected into the cell to attain the required pressure, accomplished through the combined use of a back-pressure regulator and a pressure transducer.[31] Once the data logger was activated to monitor the reaction progress, the stirrer was set in motion at a speed of 220 rpm. As hydrates began to form within the reactor, the pressure gradually declined until it stabilized, signifying a constant pressure within the cell.

2.4. Measurement Uncertainty. The uncertainty of pressure and temperature was determined and reported as combined expanded uncertainty. The contributing factors considered were instrumental errors, correlation offset, calibration errors, and an offset in repeatability. The pressure and temperature measurements yielded expanded uncertainties of 0.01 MPa and 0.1 K, respectively. The uncertainty for time was due to the instrument utilized and was 0.01 s. These parameters were utilized in the kinetic models to obtain the kinetics of gas hydrate formation, which are presented and discussed in Section 4. The expanded mass uncertainty for the solution concentration was 0.06 wt %.

3. KINETIC MODEL

The experimental data obtained in the CO_2 hydrate formation were then applied to a kinetic model. The following equations were used to determine the kinetic parameters like water-to-hydrate conversion, CO_2 gas consumption, hydrate formation rate, and storage capacity (SC).[31−34]

The rate of gas used $r(t)$ during hydrate formation was obtained by (eq 1)

https://doi.org/10.1021/acs.iecr.3c04061
Ind. Eng. Chem. Res. 2024, 63, 3867−3879

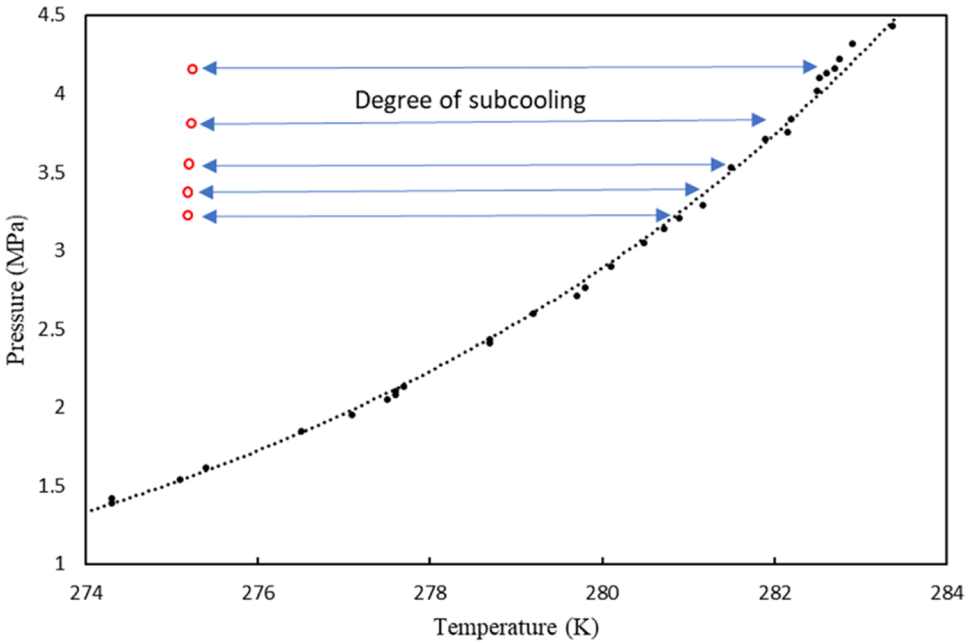

Figure 2. Degree of subcooling between the CO_2 hydrate equilibrium line and the initial kinetic experimental conditions.

Table 2. Induction Time for the Formation of the CO_2 Gas Hydrate in the Presence of Different Additives Utilized in the Study[1]

reactant	concentration of additives/wt %					
	0	0.1	0.2	0.5	1	1.2
	induction time/min					
Deionized water	8.97					
CuO + 0.05 wt % SDS solution		0.01	0.70	0.93	0.53	0.63
Al_2O_3 + 0.05 wt % SDS solution		1.70	0.87	1.03	0.73	2.03
GPN + 0.05 wt % SDS solution		0.03	0.47	0.40	38.67	32.67
C−C + 0.05 wt % SDS solution		0.01	0.10	0.93	0.77	0.83
ZnO + 0.05 wt % SDS solution		12.3	1.43	0.70	0.80	0.50
$H_{12}MgN_2O_{12}$ + 0.05 wt % SDS solution		0.67	1.53	0.7	52.13	6.23

[1]Uncertainty $U(P)$ = 0.01 MPa, $U(T)$ = ± 0.1 K, $U(t)$ = 0.01 s, and $U(x)$ = 0.06 wt %.

$$r(t) = \frac{n_{CO_{2,i-1}} - n_{CO_{2,i+1}}}{(t_{i+1} - t_{i-1})_{n_{wo}}} \quad (1)$$

where $n_{CO_{2,i-1}}$ and $n_{CO_{2,i+1}}$ are the number of moles of CO_2 in the gas phase at t_{i-1} and t_{i+1}, respectively, which are computed by the real gas law and n_{wo} is the number of moles of water at the beginning of the hydrate formation process.

Th apparent rate constant of the eq (2) was utilized.

$$k_{app} = \frac{r(t)}{f^G_{CO_2} - f^G_{equilib}} \quad (2)$$

where $f^G_{equilib}$ is the gas fugacity at the hydrate equilibrium pressure ($P_{equilib}$) and initial temperature conditions. $f^G_{equilib}$ may be estimated under equilibrium gas hydrate conditions by using the thermodynamic model.

The storage capacity is defined as the standard volume of gas stored per volume of the hydrate obtained by eq (3)

$$SC = \frac{V_{STP}}{V_H} = \frac{n_{CO_2} RT_{STP}/P_{STP}}{V_H} \quad (3)$$

The volume of gas hydrate is indicated by the subscript V_H, and STP is for standard conditions.

The water-to-hydrate conversion as the quantity of water converted to hydrate per mole of feed is computed by eq (4)

$$\text{water to hydrate conversion} = \frac{M \times \Delta n_{co_2}}{n_{w_o}} \quad (4)$$

where M is the hydration number.[32] For in-depth development of the model and equations employed in this research to calculate kinetic parameters like water-to-hydrate conversion, CO_2 gas consumption, hydrate formation rate, and storage capacity (SC), the reader is referred to the published literature works of Ndlovu,[31] Babaee et al.,[32] Fakir et al.,[33] Klauda, and Sandler.[34]

4. RESULTS AND DISCUSSION

4.1. Kinetics of Hydrate Formation. The study provided data on the kinetics of CO_2 hydrate formation, including water-to-hydrate conversion, storage capacity, gas consumption, and the gas uptake rate. The temperature and pressure operating conditions investigated for CO_2 gas hydrate formation with deionized water were 275.25−276.26 K (under a constant pressure of 4.07 MPa) and 3.32−3.41 MPa (at a constant temperature of 275.8 K), respectively.

https://doi.org/10.1021/acs.iecr.3c04061
Ind. Eng. Chem. Res. 2024, 63, 3867−3879

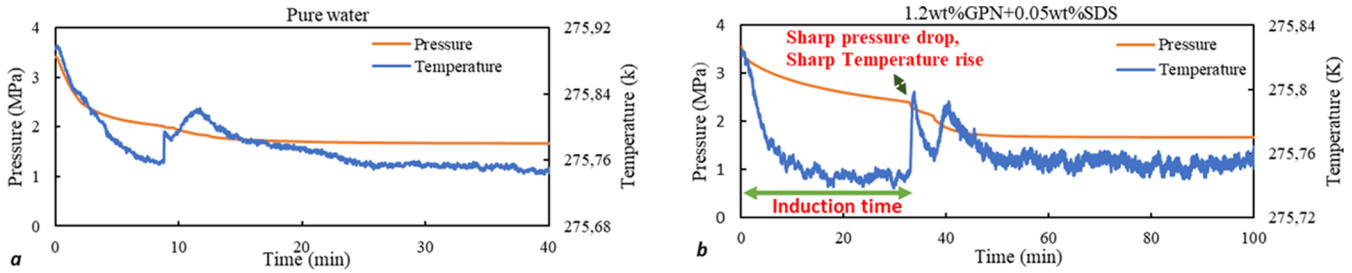

Figure 3. Induction time obtained from temperature and pressure plot for (a) Deionized water and (b) 1.2 wt % GPN + 0.05 wt % SDS.

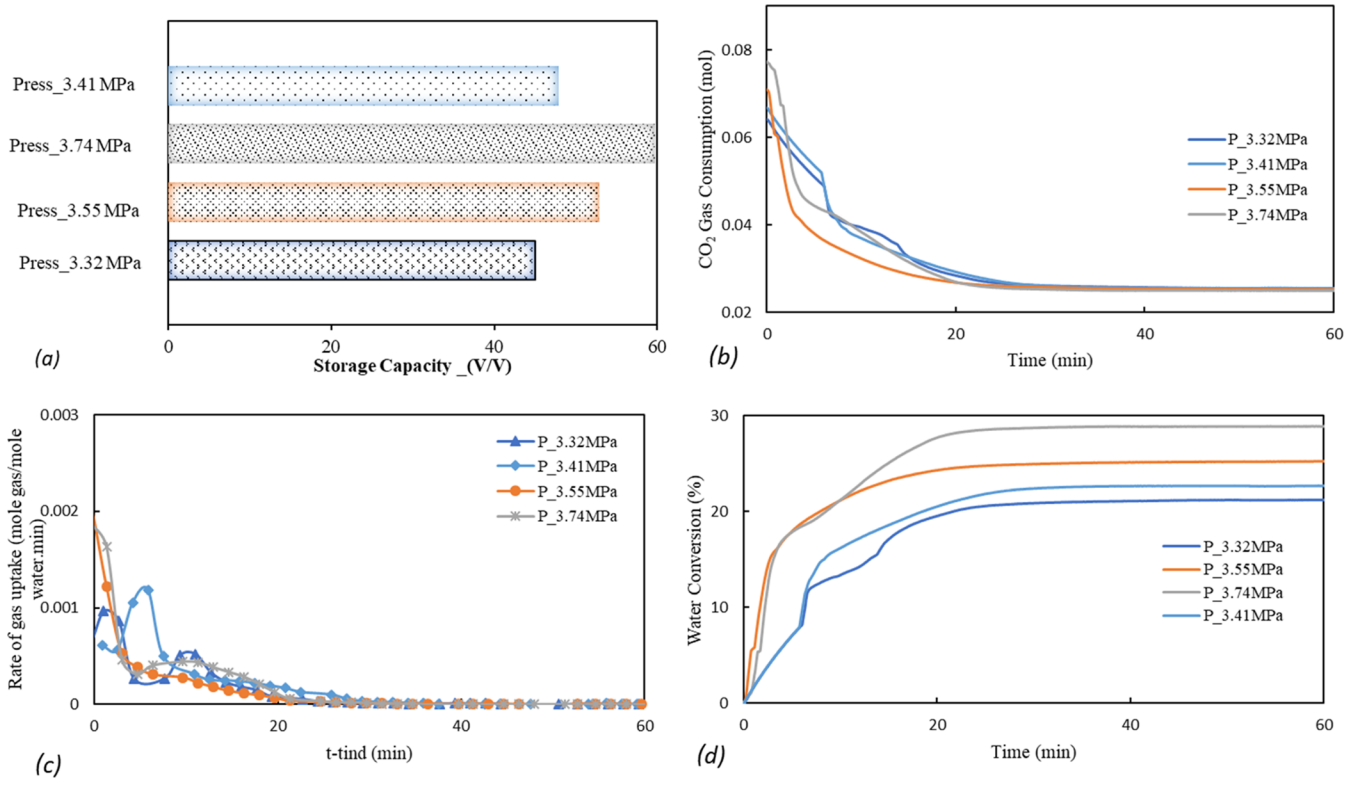

Figure 4. Pressure variation for CO_2 gas hydrate formation at a temperature of 275.8 K with Deionized water on (a) storage capacity, (b) gas consumption, (c) mol of gas consumed to mole of water, and (d) water consumed.

An important factor in the formation of hydrate clathrate is the driving force, which is the level of subcooling. This is a measure of the pressure discrepancy from the initial pressure to the equilibrium point. As depicted in Figure 2, elevating the initial CO_2 pressure leads to a greater level of subcooling and accelerates the formation of gas hydrates.[31] The experimental hydrate dissociation data points acquired in this study were precisely located on the equilibrium curve. This alignment serves as a confirmation that both the equipment and the experimental procedure employed in the investigation were well suited and reliable for the intended purposes. The data points' coincidence with the equilibrium curve attests to the accuracy and precision of the experimental setup, providing a solid foundation for the validity and credibility of the results obtained.

4.2. Induction Time. The time taken for induction is a critical factor in the process of hydrate nucleation.[23,35] In this study, the induction time for all of the investigated systems is detailed in Table 2.

Figure 3(a,b) displays the time-based temperature and pressure profiles during CO_2 hydrate formation in the presence of deionized water and 1.2 wt % graphene +0.05 wt % SDS solution in order to show how induction time was determined using these two systems. The induction time is illustrated by a rapid rise in temperature on the temperature−time graph and a minor drop in system pressure on the pressure−time graph, indicating the encapsulation of gas into the hydrate. This phenomenon is clearly depicted in Figure 3(b).

According to Table 2, which summarizes the study's findings, it can be seen that nanoparticle concentration must fall between certain bounds in order to improve gas development, which impacts the rate at which hydrate formation occurs. There is an upper limit, where agglomeration may occur and impair the mass and heat transmission required for hydrate formation, and a lower limit, where the additions have little to no impact on hydrate formation. These behaviors differ for different additives. In an experimental investigation to assess the effects of kinetic additive on CO_2 capture in gas hydrates, Cheng et al.,[35] observed that 10 wt % TBAB and 0.2 wt % SiO_2 nanoparticles systems reduced the induction time by 53.5%, the 19 wt % had the shortest induction time of 64.7 minutes. Based on this study, it can be deduced that high

https://doi.org/10.1021/acs.iecr.3c04061
Ind. Eng. Chem. Res. 2024, 63, 3867−3879

Table 3. Summary of the Kinetic Parameters Obtained from Experimental Measurements in the Study[a]

initial temperature (K)	initial pressure (MPa)	stirring speed (rpm)	aqueous solution	storage capacity (V/V)	water conversion (%)	rate of gas uptake mol of gas/mol of water	moles of CO_2 consumed (mol)
275.80	3.74	220	water	**59.70**	**28.90**	0.0019	**0.050**
275.25	4.07	220	water	19.26	8.63	0.0007	0.010
275.75	4.07	220	water	14.79	6.30	**0.0029**	0.009
275.80	3.41	220	1.2 wt % GPN + 0.05 wt % SDS	**51.00**	**24.98**	0.0008	0.044
275.80	3.41	220	0.2 wt % GPN + 0.05 wt % SDS	47.90	22.89	0.0024	**0.044**
275.80	3.41	220	1.2 wt % C−C + 0.05 wt % SDS	48.10	22.98	**0.0024**	0.041

[a]Uncertainty $U(t)$ = 0.01 s, $U(T)$ = ± 0.1 K, U (x%) = 0.06 wt %, $U(P)$ = 0.01 MPa best-performing system is presented in bold.

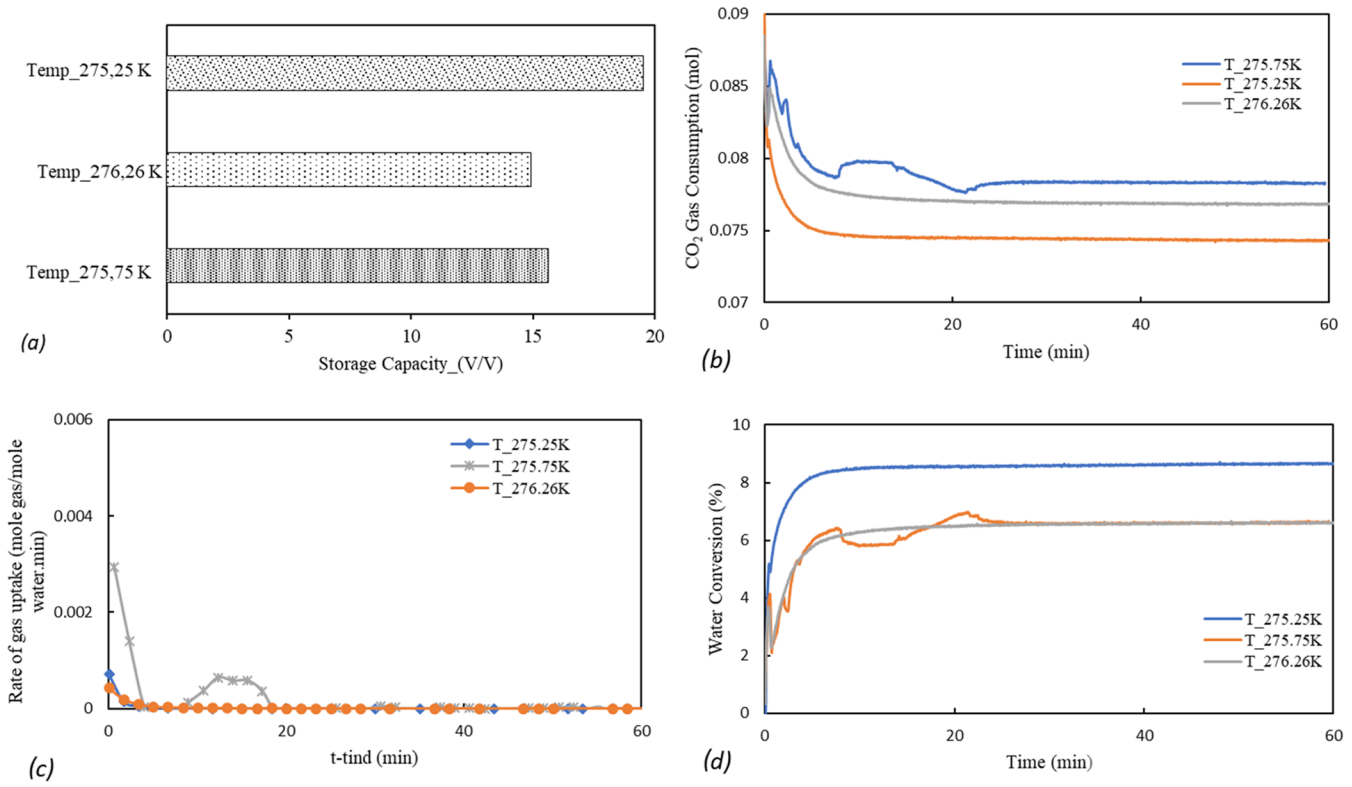

Figure 5. Temperature variation for CO_2 gas hydrate formation at a pressure of 4.07 MPa with deionized water on (a) storage capacity, (b) gas consumption, (c) mol of gas consumed to mole of water, and (d) water consumed.

concentrations of addictive lead to a longer induction time. Zhou et al.,[24] operating at 277.15 K and 4.5 MPa reported that 0.4 wt % graphite nanoparticles reduced the induction time from 32.5 minutes to 7 minutes which was higher than the values obtained in this study which might be attributed to the absence of SDS in the literature study. Liu et al.,[36] obtained the best induction time of 40 minutes when 0.0025 wt % GO (graphene oxide) was added to a carbon dioxide-on this study, it can be deduced that high concentrations of addictives lead to a longer induction time. Zhou et al.,[24] operating at 277.15 K and 4.5 MPa reported that 0.4 wt % graphite nanoparticles reduced the induction time from 32.5 minutes to 7 minutes which was higher than the values obtained in this study which might be attributed to the absence of SDS in the literature study. Liu et al.,[36] obtained the best induction time of 40 minutes when 0.0025 wt % GO (graphene oxide) was added to a carbon dioxide-water system.

4.3. Pressure Variation. The impact of pressure fluctuations on the kinetics of CO_2 hydrate formation was examined. Multiple experiments were conducted with initial pressures set at 3.32, 3.41, 3.55, and 3.74 MPa while maintaining a consistent initial temperature of 275.8 K.[31] Throughout the pressure variation phase, CO_2 hydrate formation was conducted using deionized water without additional substances. The experimental assessments encompassed four key factors: storage capacity, the ratio of gas moles to water moles, the water conversion percentage, and gas consumption. Figure 4(a) through Figure 4(d) demonstrates that favorable outcomes were achieved across all four examined parameters when the pressure was elevated from 3.32 to 3.74 MPa. As a result, high pressures were shown to be favorable for the production of gas hydrates, as documented in literature studies.[37] Nevertheless, the high-pressure production of gas hydrates is prohibitively expensive, rendering them economically unviable for various applications. Consequently, the use of chemicals to augment hydrate formation under low-pressure conditions becomes imperative.

Figure 4(a) demonstrates that the highest pressure, 3.74 MPa, produced a maximum of 59.7 (v/v), while the lowest pressure, 3.32 MPa, produced the lowest storage capacity of

https://doi.org/10.1021/acs.iecr.3c04061
Ind. Eng. Chem. Res. 2024, 63, 3867−3879

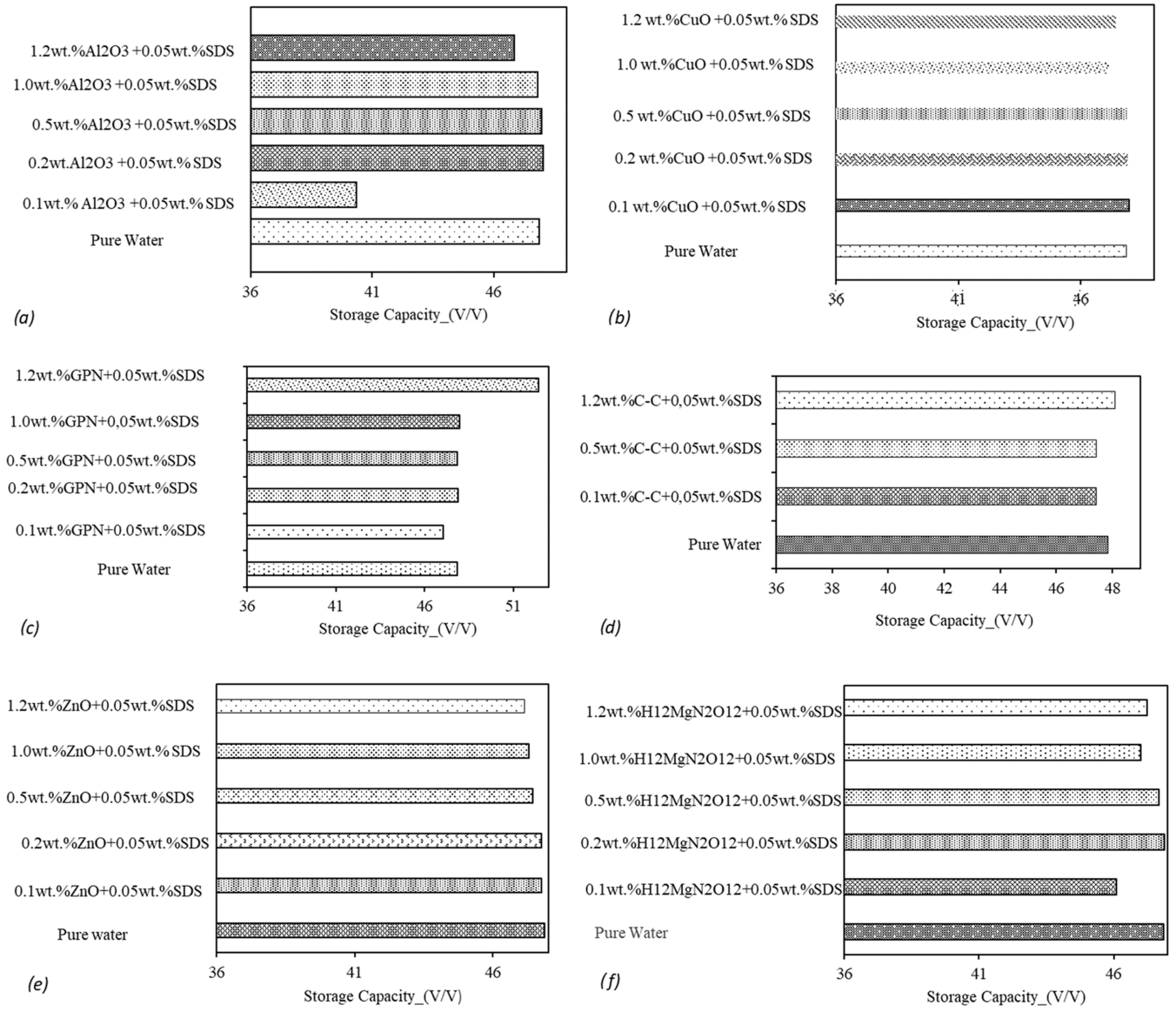

Figure 6. Storage capacity of formed CO_2 hydrate at an initial pressure of 3.41 MPa and initial temperature of 275.8 K for the following systems: (a) Al_2O_3 nanoparticles, (b) CuO nanoparticles, (c) graphene nanoplatelets, (d) graphite powder, (e) ZnO powder, and (f) $H_{12}MgN_2O_{12}$.

44.8 (v/v). From 3.32 to 3.74 MPa, storage capacity increased with pressure. Thus, the capacity of the hydrate to store gases was observed to be directly proportional to the initial pressure.

Gas consumption exhibited similar levels across the four pressures, as indicated in Figure 4(b). Within the pressure range of 3.32−3.74 MPa, a maximum of 0.05 mol of gas was utilized. The ratio of gas moles to water moles is illustrated in Figure 4(c). The highest value, 0.05 mol/mol, was achieved at 3.74 MPa, while the lowest value, 0.00061 mol/mol, was observed at 3.41 MPa. The number of moles increased with the rise in pressure from 3.35 to 3.74 MPa in a similar fashion. Table 3 is a summary of the performance of various additives tested in this work.

Figure 4(d) displays the water conversion percentage, varying from a peak of 28.9% at 3.74 MPa to a low peak of 21.2% at 3.22 MPa. This conversion percentage exceeds that reported by Fakir et al.,[33] who noted a maximum conversion of slightly under 8% at a pressure of 3.20 MPa using deionized water. For gas hydrate experiments, there is an increase in water consumption with an increase in pressure (specific pressure range).[38]

4.4. Temperature Variations. Temperature variation tests were carried out at a pressure of 4.07 MPa. The temperature varied from 275.25 to 276.26 K, and it was discovered that both 275 and 276.26 K produced the same performance. Figure 5(a−d) shows the improvement in hydrate formation kinetics as temperature decreased, with the best results being attained at 275.25 K, the lowest temperature. Based on Figure 5(a), the highest and lowest storage capacities (SC) are 19.26 and 14.76 (v/v) at temperatures of 275.25 and 276.26 K, respectively. For the gas consumption, Figure 5(b) indicates the maximum value of 0.01 mol, which occurred at 275.25 K. Conversely, the lowest gas consumption was observed at 275.75 K. The best outcome was obtained with a ratio of 0.0029 mol/mol for moles of gas consumed to moles of water and is depicted in Figure 5(c) at a temperature of 275.75 K. The water conversion percentage was less than 10% for all of the temperatures investigated, as shown in Figure 5(d), showing poor hydrate formation.[28]

https://doi.org/10.1021/acs.iecr.3c04061
Ind. Eng. Chem. Res. 2024, 63, 3867−3879

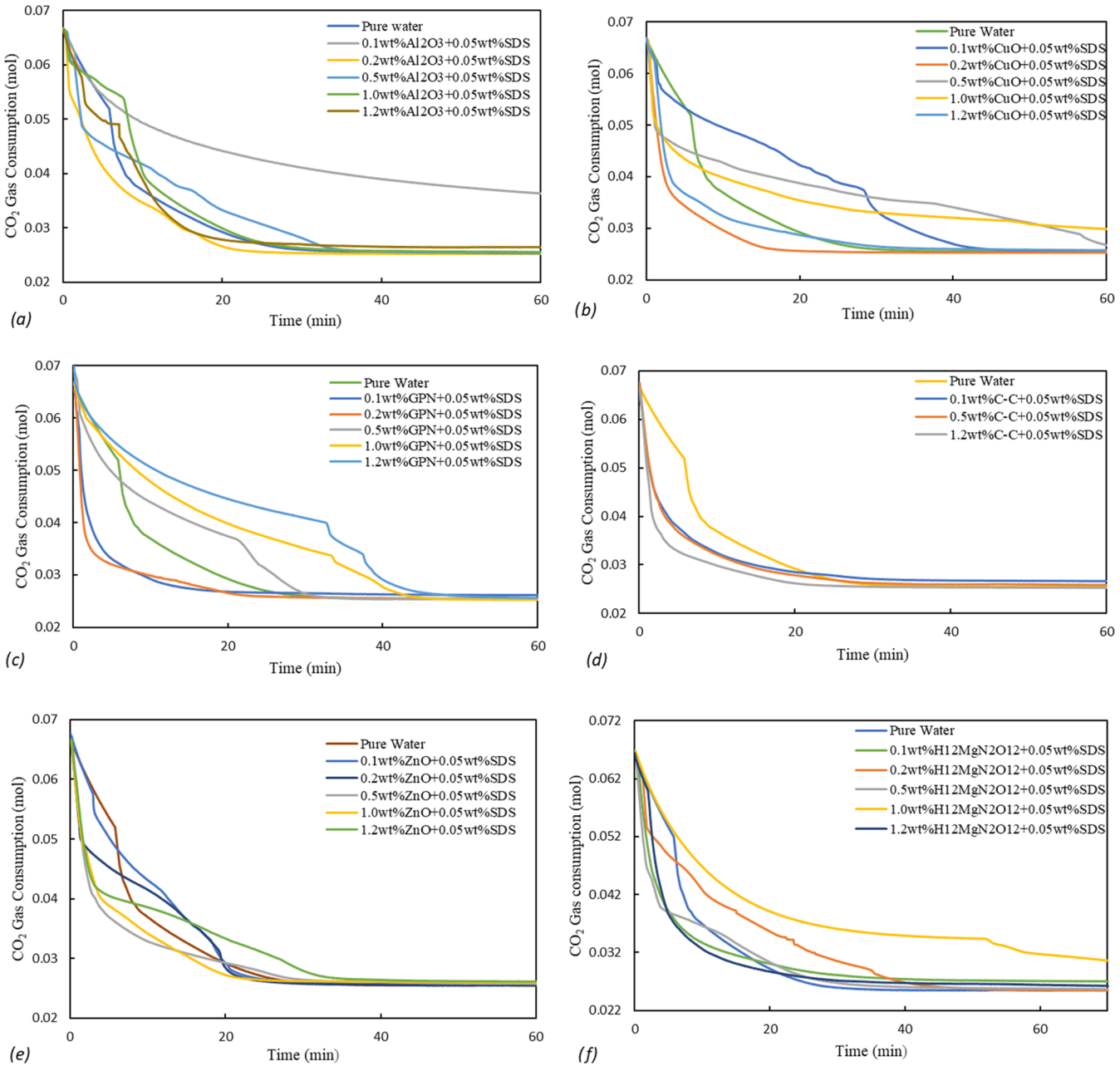

Figure 7. Carbon dioxide consumed during hydrate formation at an initial temperature of 275.8 K and an initial pressure of 3.41 MPa in the presence of (a) Al_2O_3 nanoparticles, (b) CuO nanoparticles, (c) graphene (GPN) nanoplatelets, (d) graphite (C−C) powder, (e) ZnO powder, and (f) $H_{12}MgN_2O_{12}$ crystals.

4.5. Additives Kinetics. *4.5.1. Storage Capacity.* Figure 6(a−f) reports the capacity of gas hydrates to store CO_2 with the use of additives. A clustered bar graph was used to present the maximum value of the gas stored for the different additives used in the investigation. The quantity of gas that a hydrate lattice can hold is indicated by its storage capacity, which is an important consideration when researching hydrates for carbon capture and gas storage. The study yielded an average storage capacity of 47 v/v for all solutions examined. However, the highest storage capacity, 52 (v/v), was achieved using a combination of 1.2 wt % GPN and 0.05 wt % SDS. Conversely, the lowest reported storage capacity was 35.49 (v/v), which was achieved with 0.1 wt % Al_2O_3 and 0.05 wt % SDS. This highlights the favorable effect of nanoparticles on CO_2 storage, as they were able to store a greater amount of gas in the deionized solution. Firoozabadi et al.,[20] observed that the storage capacity of CO_2 gas hydrate increased from 10.9 (v/v) for a pure water system to 25.5 (v/v) with 0.15 wt.% Fe_3O_4 and further to 43.8 (v/v) when a magnetic field was applied to the system. This investigation was carried out at 3 MPa and 274.15 K. As expected, the storage capacity was found to increase as the pressure was raised. This storage capacity obtained with nanofluids was in the same range as the one from the study, the magnetic field provided a technic which served to improve it.

4.5.2. Gas Consumption. The quantification of gas consumption in the production of CO_2 hydrate in this research was determined by measuring the rate at which the gas entered the hydrate phase. Figure 7(a−f) presents the gas consumption during the formation of the CO_2 hydrate with

https://doi.org/10.1021/acs.iecr.3c04061
Ind. Eng. Chem. Res. 2024, 63, 3867−3879

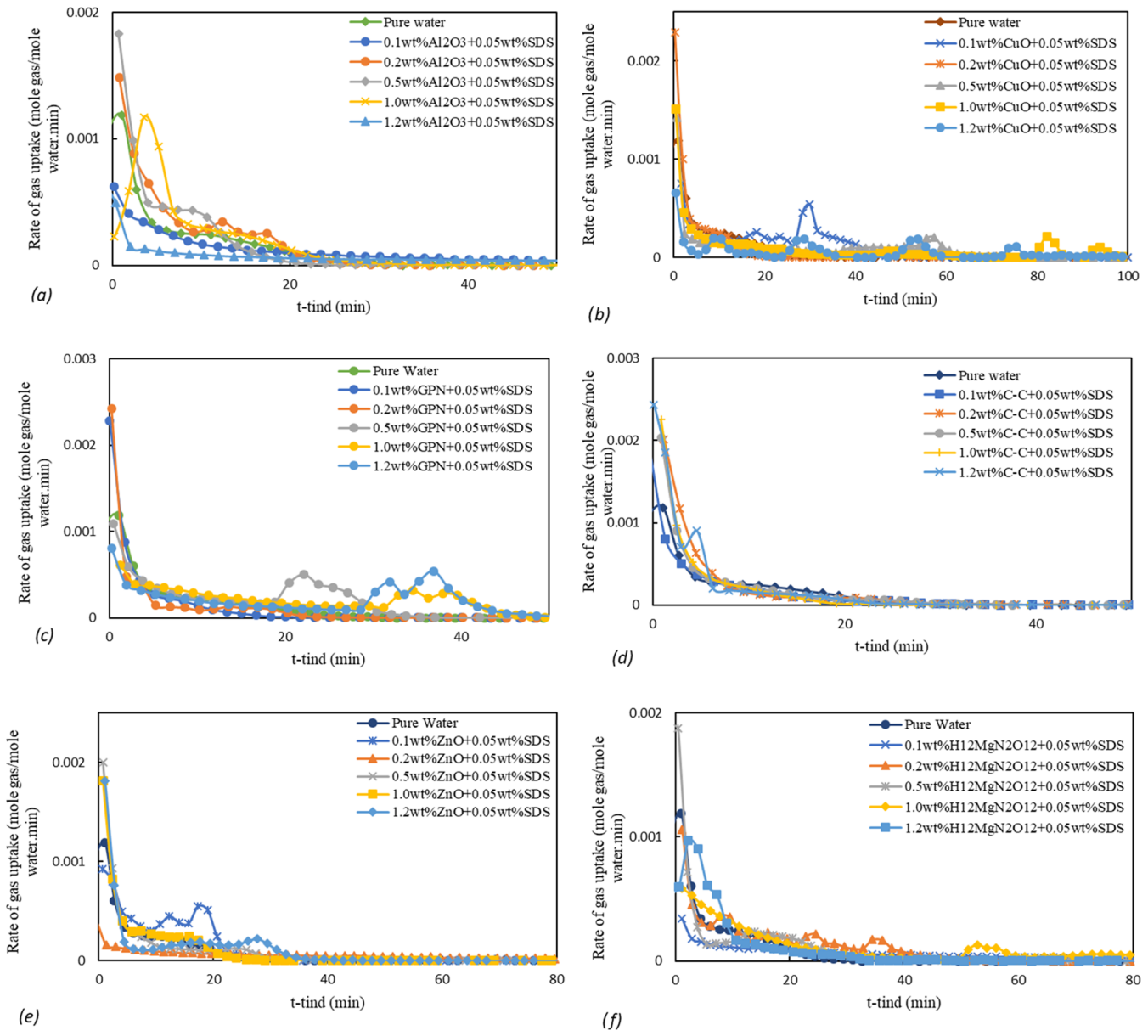

Figure 8. Rate of CO_2 consumption during hydrate formation at a temperature of 275.8 K and pressure of 3.41 MPa in concentrations specified in the presence of (a) Al_2O_3 nanoparticles, (b) CuO nanoparticles, (c) graphene (GPN) nanoplatelets, (d) graphite (C−C) powder, (e) ZnO powder, and (f) ($H_{12}MgN_2O_{12}$) crystals.

various additives. Specifically, Figure 7(a) illustrates the reduction in CO_2 gas consumption as gas hydrate forms in the presence of Al_2O_3 nanoparticles alongside 0.05 wt % SDS. At the initial stage of the reaction, there is a rise in the rate of gas consumption. This is evident in the graph, particularly between 0.2 and 1.2 wt % of Al_2O_3. In the presence of different concentrations of Al_2O_3, it is observed that CO_2, except for the system with 1.0 wt % Al_2O_3, was consumed more quickly than deionized water. Despite this, the final gas consumption for each concentration used was 0.0389 mol. With 0.1 wt % Al_2O_3, an anomaly with a gas consumption of 0.025 mol was observed. This experimental run was repeated to confirm this observation. This outcome may have been caused by the small concentration of Al_2O_3 in the solution to effect a change in the reaction conditions. Figure 7(b) displays the patterns observed with CuO nanoparticles with an average CO_2 consumption of 0.0382 mol across all concentrations investigated. By examining the slopes of the graphs, it becomes evident that the reaction rate surpassed that achieved with Al_2O_3 nanoparticles. The highest performance was demonstrated by graphene nanoplatelets, which used 0.0437 mol of gas at a concentration of 0.1 wt %.

The nanoparticle system had a faster reaction rate compared to the water system. As depicted in Figure 7(d), when utilizing graphite powder, the rate of gas consumption exceeded that of pure water across all concentrations, resulting in an overall gas consumption of 0.039 mol. Gas consumption trends are shown in Figure 7(e,f) for zinc oxide and magnesium nitrate hexahydrate. Both systems demonstrated an improved performance in comparison to deionized water, with an average gas consumption of 0.038 mol.

4.5.3. Rate of Gas Uptake (Mole of Gas/Mol of Water). In Figure 8(a−f), the gas absorption rate was graphed over time as CO_2 hydrate formed in the presence of nanoparticle

https://doi.org/10.1021/acs.iecr.3c04061
Ind. Eng. Chem. Res. 2024, 63, 3867−3879

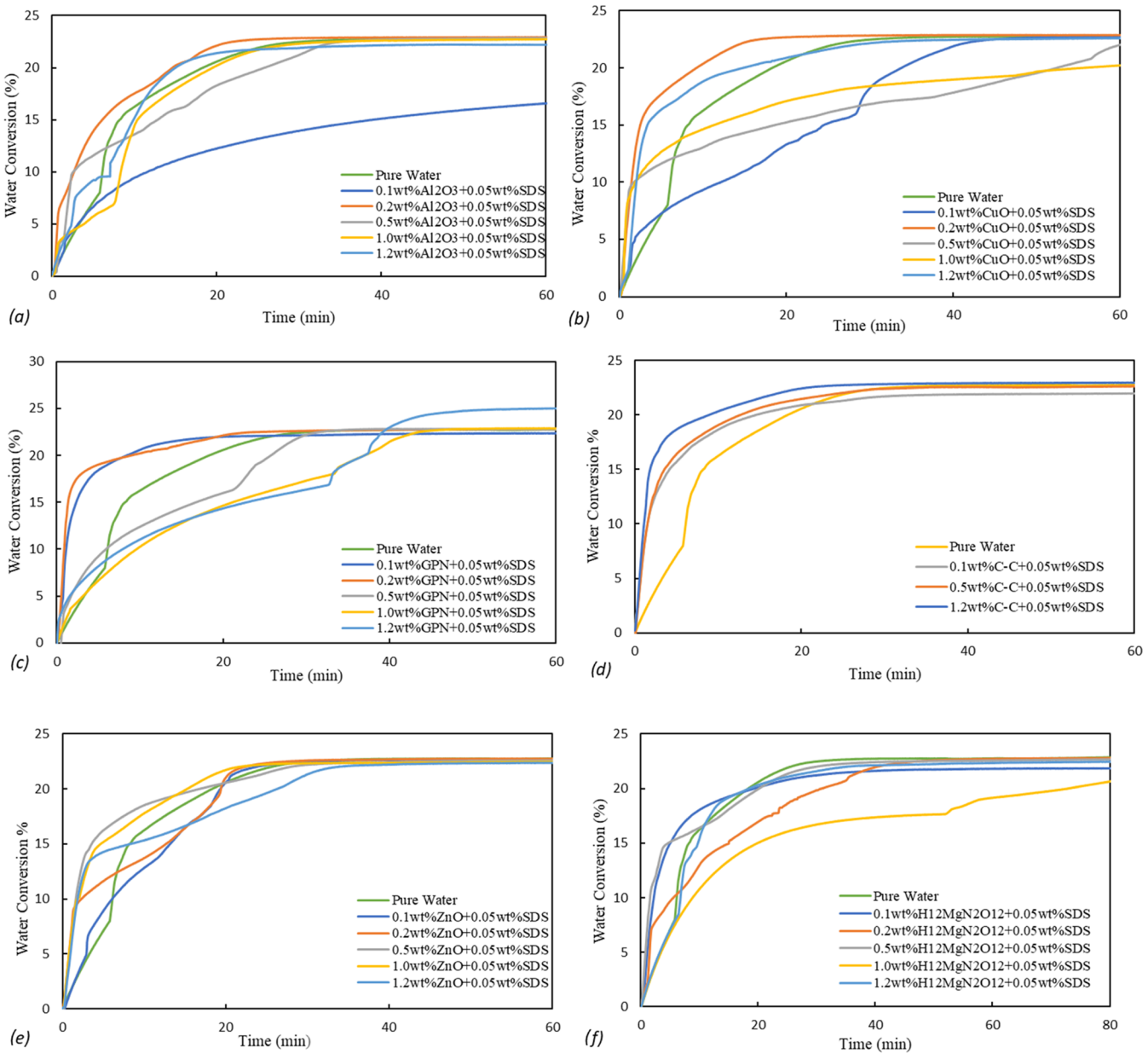

Figure 9. Water conversion % in CO_2 hydrate at a pressure of 3.41 MPa and temperature of 275.8 K in the presence of (a) Al_2O_3 nanoparticles, (b) CuO nanoparticles, (c) graphene (GPN) nanoplatelets, (d) graphite (C−C) powder, (e) ZnO powder, and (f) magnesium nitrate hexahydrate ($H_{12}MgN_2O_{12}$) crystals.

solutions at concentrations ranging from 0.1 to 1.2 wt %, along with 0.05 wt % SDS.

Figure 8 shows that in all of the tested systems, in the presence of nanofluids, the gas consumption rate surpassed that of pure water (deionized water). This is evidenced by the initial spike in values attributed to the elevated concentration of reactants at the onset of the reaction. Thus, from reaction kinetics, the higher the concentration of the reactant, the more frequent the bombardment of reactants against each other, making the rate of reaction faster. The reaction rate decreases as the concentration of the reactants is being used up. In this study, the reaction followed a similar reaction profile, as the concentration of nanoparticles decreased the reaction rate decreased in a similar manner. When compared to other systems with chemical additions, the nanoparticles exhibit a higher rate of gas uptake. The highest obtained value was 2.44 $\times 10^{-3}$ mol G/(mol W min) with graphite powder at 1.2 + 0.05 wt % SDS. Figure 8(a−c) shows that a rate constant for nanoparticle is higher than 2.0×10^{-3} mol G/(mol W min), except for Al_2O_3 nanoparticles with the rate of gas uptake (mole of gas/mol of water) of 2.4×10^{-3} mol G/(mol W min) obtained with 0.2 wt % graphite nanoparticles and 1.2 wt % graphite powder. In contrast, for ZnO and $H_{12}MgN_2O_{12}$ depicted in Figure 8(e,f), the rates of gas absorption were comparatively lower, with their peak values being below 2.0×10^{-3} mol G/mol W min. Figure 8 illustrates that the rate of gas absorption was fast at low nanoparticle concentrations of 0.1 and 0.2 wt % but declined, as the weight percent was increased. This was ascribed to the solution being saturated, which prevented the reactants from making effective contact with one another. As depicted in Figure 8(f), the reaction rate of magnesium nitrate hexahydrate proved to be faster than

https://doi.org/10.1021/acs.iecr.3c04061
Ind. Eng. Chem. Res. 2024, 63, 3867−3879

initially anticipated. Surprisingly, the overall consumption of magnesium nitrate hexahydrate was in the same range as that of the nanoparticles.

4.5.4. Water Conversion Percentage. Figure 9(a–f) depict the patterns of percentage water conversion throughout the CO_2 hydrate formation process carried out in this investigation. As is evident from the figures, the water conversion aligns with the trends observed in gas consumption during hydrate formation.

The highest water conversion, averaging 22.72%, was attained across all of the examined systems, except for the configuration with 1.2 wt % GPN + 0.05 wt % SDS, which achieved a maximum water conversion of 25%. This represented the highest water conversion observed in the entire study. According to Loveday et al.,[39] gas hydrates are nonstoichiometric crystalline structures comprising small gas molecules and water molecules confined within the clathrate lattice, in approximately 85% water and 15% gas. Therefore, substantial water conversion allows for a significant volume of gas to be encapsulated within the hydrate lattice. This could hold potential advantages for employing gas hydrates in gas storage and CO_2 capture applications. The water-to-hydrate conversion reported by Firoozabadi et al. [20] increased from 5.7 (mole/mole) for a pure water system to 14.5% (mol/mole) for a 0.07 wt.% Fe_3O_4. This amount was further increased to 36 (mol/mol) when a magnetic field was applied. The amount obtained with 0.07 wt.% Fe_3O_4 in the absence of a magnetic field was lower than that reported in this study mainly due to surface tension which existed between the nanoparticles and the solution. In this study, SDS was added to cater for this effect.In general, the results obtained in this investigation on the capture of carbon dioxide and storage are comparable to results that have been published by Said et al.[23] and Mohammadi et al.[15] The notable difference is in storage capacity, which is caused by different mathematic models utilized by different researchers.

5. CONCLUSIONS

Research into the kinetic parameters affecting gas hydrate formation such as storage capacity, induction time, gas consumption, water conversion percentage, and the ratio of gas consumed to moles of water was performed. Nanofluids containing additive concentrations ranging from 0.1 to 1.2 wt %, along with 0.05 wt % SDS, were employed to examine their influence on the kinetics of CO_2 hydrate formation. Across all experiments involving additives, the initial conditions were standardized at 275.8 K and 3.41 MPa for pressure and temperature, respectively. The findings of this study affirm the beneficial effect of additives and underscore the advantageous effects of nanoparticles on the kinetics of the formation of CO_2 hydrate clathrate formation.

The experimental results demonstrate that nanoparticles enhance the kinetics of CO_2 gas hydrate formation, yielding a maximum storage capacity of 51 (v/v). This was achieved using a nanofluid containing 1.2 wt % graphene nanoplatelets, while the lowest storage capacity of 35 (v/v) was observed with a 0.1 wt % aluminum oxide nanofluid. In terms of water conversion, the nanofluid containing 1.2 wt % graphene nanoplatelets exhibited a peak value of 25%, whereas the lowest value of 16% was obtained using the 0.1 wt % aluminum oxide nanofluid solution. Regarding induction time, the introduction of nanoparticles and graphite led to a significant reduction, with most concentrations resulting in less than 1 min. The induction time dropped from 9 min to under 1 min when CuO and Al_2O_3 nanoparticles were introduced. However, with the use of ZnO and $H_{12}MgN_2O_{12}$ nanoparticles, the induction time increased by more than 10 min. Among the concentrations studied, graphite powder at 1.2 wt % demonstrated the highest rate of gas absorption, registering at 0.0024 (mol of gas/mol of water min). Conversely, the lowest gas uptake was recorded at 0.0003 (mol of gas/mol of water min), which was achieved with 0.1 wt % magnesium nitrate hexahydrate. Results obtained in this investigation are favorable for the use of nanoparticles in CO_2 gas storage in gas hydrates. Overall, the 1.2 wt % graphene nanoparticles +0.05 wt % SDS system was deemed to be ideal for utilization in CO_2 capture and storage as it had the highest storage capacity, water conversion percentage, and moles of CO_2 consumed compared to other systems investigated.

The capacity of hydrates to swiftly capture CO_2 is an advantageous feature, as it leads to a notable reduction in the reaction duration, ultimately enhancing process efficiency. The augmented storage capacity facilitated by nanoparticles in the CO_2 storage analysis is pivotal in ensuring a substantial amount of gas is securely stored within the hydrate. This reservoir of gas can be effectively utilized for purposes like storage and transportation. Furthermore, a fairly higher amount of gas consumption shown by nanoparticles makes it desirable for application in hydrate for gas storage. The concentration variation of the additives did not show much effect on the parameters investigated. The highest pressure utilized in the study had the best results in all of the variables investigated in pressure variation. However, such higher pressures are often undesirable for practical applications due to increased operational costs and equipment design strengths, though the presence of nanoparticles in gas hydrates shows promising behaviors and improved kinetic properties for CO_2 gas capture and storage.

■ ASSOCIATED CONTENT

Supporting Information

The Supporting Information is available free of charge at https://pubs.acs.org/doi/10.1021/acs.iecr.3c04061.

[Repeatability and reproducibility of data in CO_2 Kinetic measurements] to check the reliability of the equipment and procedure; before the commencement of the kinetic measurements, CO_2 hydrate phase equilibrium data was measured and compared with the available experimental data in the literature; this information is available in Figures S.1 and S.2; in addition, the readability of the kinetic measurements was shown through repeating induction times for three distinct systems; which are presented in Figures S.3–S.5; along with a summarized presentation in Table S.2; this comprehensive verification process establishes a strong foundation for the subsequent kinetic measurements; enhancing the overall reliability and precision of the study (PDF)

■ AUTHOR INFORMATION

Corresponding Author

Saeideh Babaee − *Department of Chemical and Metallurgical Engineering, University of the Witwatersrand, Johannesburg 2000, South Africa;* orcid.org/0000-0003-2412-8618; Email: saeideh.babaee@witz.ac.za

https://doi.org/10.1021/acs.iecr.3c04061
Ind. Eng. Chem. Res. 2024, 63, 3867−3879

Authors

Phakamile Ndlovu − *Thermodynamics Research Unit, School of Engineering, University of KwaZulu-Natal, Durban 4041, South Africa; Minerals Processing Division, Mintek, Randburg 2125, South Africa*

Paramespri Naidoo − *Thermodynamics Research Unit, School of Engineering, University of KwaZulu-Natal, Durban 4041, South Africa; Department of Chemical Engineering, Banhoekweg, Stellenbosch University, Stellenbosch 7600 Western Cape, South Africa;* orcid.org/0000-0002-2724-7308

Kuveneshan Moodley − *Thermodynamics Research Unit, School of Engineering, University of KwaZulu-Natal, Durban 4041, South Africa;* orcid.org/0000-0003-1544-3624

Complete contact information is available at: https://pubs.acs.org/10.1021/acs.iecr.3c04061

Notes

The authors declare no competing financial interest.

■ ACKNOWLEDGMENTS

The Thermodynamics Research Unit at the School of Engineering at the University of KwaZulu Natal and the South African National Research Fund Grant UID 118606 provided funding for this study.

■ REFERENCES

(1) Solomon, S.; Qin, D.; Manning, M.; Chen, Z.; Marquis, M.; Averyt, K. B.; Tignor, M.; Miller, H. L. *IPCC () Climate Change: The Physical Science Basis EXITEXIT EPA WEBSITE. Contribution of Working Group I to the Fourth Assessment Report of the Intergovernmental Panel on Climate Change2007* C. U. Press: Cambridge, United Kingdom; 2007996.

(2) Songolzadeh, M.; Ravanchi, M. T.; Soleimani, M. Carbon Dioxide Capture and Storage: A General Review on Adsorbents. *Int. J. Chem. Mol. Eng.* **2012**, *10* (2012), 906−913.

(3) Herzog, H.; Golomb, D. Carbon Capture and Storage from Fossil Fuel Use. *Encycl. Energy* **2004**, *1* (6562), 277−287.

(4) Eslamimanesh, A.; Mohammadi, A. H.; Richon, D.; Naidoo, P.; Ramjugernath, D. Application of gas hydrate formation in separation processes: A review of experimental studies. *J. Chem. Thermodyn.* **2012**, *46*, 62−71.

(5) Ochedi, F. O.; Yu, J.; Yu, H.; Liu, Y.; Hussain, A. Carbon dioxide capture using liquid absorption methods: a review. *Environ. Chem. Lett.* **2021**, *19*, 77−109.

(6) IEA. *Towards Zero Emission Coal-fired Power Plants Clean Coal Centre, Report CC/101*, 2005.

(7) Mondal, M. K.; Balsora, H. K.; Varshney, P. Progress and trends in CO2 capture/separation technologies: A review. *Energy* **2012**, *46*, 431−441.

(8) Wang, X.; Song, C. Carbon capture from flue gas and the atmosphere: A perspective. *Front. Energy Res.* **2020**, *8*, No. 560849, DOI: 10.3389/fenrg.2020.560849.

(9) Ndlovu, P.; Babaee, S.; Naidoo, P. Experimental study of CH4-CO2 replacement in gas hydrates in the presence of nitrogen and graphene nanoplatelets. *J. Mol. Liq.* **2023**, *371*, No. 121109.

(10) Xu, C. G.; Chen, Z. Y.; Cai, J.; Li, X. S. Study on Pilot-scale CO2 separation from flue gas by the hydrate method. *Energy Fuels* **2014**, *28*, 1242−1248.

(11) Koh, C. A.; Sum, A. K.; Sloan, E. D., JrClathrate hydrates of carbon dioxide *Rev. Mineral. Geochem.* 2011; Vol. 75 1, pp 289−314.

(12) Majumder, A. K.; Ramakrishnan, T. S.; Padmakumar, K.; Rao, D. N.Formation conditions of nitrogen hydrates: Experimental investigations and modelling *J. Nat. Gas Sci. Eng.* 2018; Vol. 57, pp 39−49.

(13) Huang, J.; Liang, D.; Li, H.; Cui, W.; Liu, C.; Li, Y.Experimental Study on Oxygen Hydrate Formation Conditions *Energy Procedia* 2016; Vol. *105*, pp 1275−1280.

(14) Lu, Y. Y.; Ge, B. B.; Zhong, D. L. Investigation of using graphite nanofluids to promote methane hydrate formation: Application to solidified natural gas storage. *Energy* **2020**, *199*, No. 117424.

(15) Mohammadi, A.; Manteghian, A.; Haghtalab, A.; Mohammadi, A. H.; Abkenar, M. R. Kinetic study of carbon dioxide hydrate formation in presence of silver nanoparticles and SDS. *Chem. Eng. J.* **2014**, *237*, 387−395.

(16) Ndlovu, P.; Babaee, S.; Naidoo, P. Review on CH4-CO2 replacement for CO2 sequestration and CH4/CO2 hydrate formation in porous media. *Fuel* **2022**, *320*, No. 123795.

(17) Seo, Y.; Lee, Y.; Lee, H.; Lee, J.; Lee, J.; Ryu, J.Enhancement of CO2 hydrate formation by silica nanoparticles *J. Phys. Chem. B* 2012; Vol. *116* 12, pp 3778−3785.

(18) Masoumi, M.; Khodapanah, M.; Bahramian, A.; Izadpanah, A.Investigation of CO2 hydrate formation in the presence of Fe2O3 nanoparticles *J. Mol. Liq.* 2018; Vol. *268*, pp 633−638.

(19) Soltanieh, M.; Golpayegani, M. R. H.; Hashemzadeh, M.Investigation of CO2 hydrate formation in the presence of TiO2 nanoparticles *J. Mol. Liq.* 2019; Vol. *275*, pp 696−703.

(20) Firoozabadi, S. F.; Bonyadi, M. A comparative study on the effects of Fe3O4 nanofluid, SDS and CTAB aqueous solution on CO2 hydrate formation. *J. Mol. Liq.* **2020**, *300*, 12251 DOI: 10.1016/j.molliq.2019.112251.

(21) Li, J.; Liang, D.; Guo, K.; Wang, R.; Fan, S. Formation and dissociation of HFC134a gas hydrate in nano-copper suspension. *Energy Convers. Manage.* **2006**, *47*, 201−210.

(22) Torré, J. P.; Dicharry, C.; Ricaurte, M.; Delphine, D. D.; Broseta, D. CO2 capture by hydrate formation in quiescent conditions: in search of efficient kinetic additives. *Energy Procedia* **2011**, *4*, 621−628.

(23) Said, S.; Govindaraj, V.; Herri, J. M.; Ouabbas, Y.; Khodja, M.; Belloum, M.; Sangwai, J. S.; Nagarajan, R. A study on the influence of nanofluids on gas hydrate formation kinetics and their potential: Application to the CO2 capture process. *J. Nat. Gas Sci. Eng.* **2016**, *32*, 95−108.

(24) Zhou, S. D.; Yu, S.; Zhao, M. M.; Wang, S. L.; Zhang, G. Z. Effects of Graphite nanoparticles on promoting CO2 hydrate formation. *Energy Fuels* **2014**, *28*, 4694−4698, DOI: 10.1021/ef5000886.

(25) Kashkouli, P. I. Thermodynamic Studies on CO2 Capture Through Gas Hydrate Formation Technology, Ph.D thesis; School of Chemical Engineering. University of KwaZulu Natal: South Africa, 2015.

(26) Lirio, C. F. d. S.; Pessoa, F. L. P.; Uller, A. M. Storage capacity of carbon dioxide hydrates in the presence of sodium dodecyl sulfate (SDS) and tetrahydrofuran (THF). *Chem. Eng. Sci.* **2013**, *96*, 118−123.

(27) Choi, J. W.; Chung, J. T.; Kang, Y. T. CO2 hydrate formation at atmospheric pressure using high efficiency absorbent and surfactants. *Energy* **2014**, *78*, 869−876.

(28) Moraveji, M. K.; Golkaram, M.; Davarnejad, R. Effects of CuO nanoparticle on dissolution of methane in water. *J. Mol. Liq.* **2013**, *180*, 45−50.

(29) Aliabadi, M.; Rasoolzadeh, A.; Esmaeilzadeh, F.; Alamdari, A. Experimental Study of Using CuO Nanoparticles as a Methane Hydrate Promoter. *J. Nat. Gas Sci. Eng.* **2015**, *27*, 1518−1522.

(30) Ngema, P. T.; Petticrew, C.; Naidoo, P.; Mohammadi, A. H.; Ramjugernath, D. Experimental measurements and thermodynamic modelling of the dissociation conditions of clathrate hydrates for (refrigerant + NaCl water) systems. *J. Chem. Eng. Data* **2014**, *59* (2), 466−475, DOI: 10.1021/je400919u.

(31) Ndlovu, P. Carbon Dioxide Encapsulation in Methane HydratesPh.D. thesisDepartment of Chemical Engineering. School of Agriculture, Science and Engineering. University of KwaZulu Natal: Durban. South Africa, 2022.

(32) Babaee, S.; Hashemi, H.; Mohammadi, A. H.; Naidoo, P.; Ramjugernath, D. Kinetic and thermodynamic behaviour of CF4 clathrate hydrates. *J. Chem. Thermodyn.* **2015**, *81*, 52−59.
(33) Fakir, T.; Babaee, S.; Naidoo, P. Application of gas hydrate for the treatment of vinasse: Phase equilibrium and kinetic investigations. *J. Chem. Eng. Data* **2021**, *66* (1), 504−514.
(34) Klauda, J. B.; Sandler, S. I. A fugacity model for gas hydrate phase equilibria. *Ind. Eng. Chem. Res.* **2000**, *39*, 3377−3386.
(35) Mohammadi, A.; Manteghian, M.; Mohammadi, A. H.; Jahangiri, A. Induction time, storage capacity, rate of methane hydrate formation in the presence of SDS and silver nanoparticles. *Chem. Eng. Commun.* **2017**, *204* (12), 1420−1427, DOI: 10.1080/00986445.2017.1366903.
(36) Liu, N.; Chen, L.; Liu, C.; Yang, L.; Liu, D. Experimental study of carbon dioxide hydrate formation in the presence of graphene oxide. *Energy* **2020**, *211*, 118994.
(37) McLeod, H. O.; Campbell, J. M. Natural Gas Hydrates at Pressures to 10,000 psia. *J. Pet. Technol.* **1961**, *13*, 590−594.
(38) Zhang, Y.; Cui, X.; Li, X.; Li, Y.; Li, J.Kinetic study on gas hydrate formation and dissociation processes with different water contents *J. Mol. Liq.* 2017; Vol. *241*, pp 1096−1102.
(39) Loveday, J. S.; Nelmes, R. J. High-pressure gas hydrates. *Phys. Chem. Chem. Phys.* **2008**, *10*, 937−950.

https://doi.org/10.1021/acs.iecr.3c04061
Ind. Eng. Chem. Res. 2024, 63, 3867−3879